Comparative Assessment of Different Computational Models for Generation of X-Ray Spectra in Diagnostic Radiology and Mammography

M. R. Ay, S. Sarkar, M. Shahriari, D. Sardari and H. Zaidi

Abstract— **The x-ray spectra predicted by different computational models used in diagnostic radiology and mammography energy range has been assessed by comparison with experimentally measured spectra. The comparative assessment encompassed many figures of merit including qualitative assessment of the spectra shape, the difference in K x-ray yield, transmission curves, Half Value Layers (HVLs) and absorbed dose and Effective Dose Equivalent (EDE) imparted to the adult ORNL hermaphroditic phantom when using x-ray spectra generated with different models at different tube voltages. The calculated spectra with X-raytbc and IPEM agreed well with measured spectra in diagnostic radiology and mammography energy range, respectively. The student's *t*-test statistical analysis showed there is no statistically significant difference between measured and generated spectra for all computational models investigated in this study. In addition, the MCNP4C-based Monte Carlo calculations showed there is no discernable discrepancy in the calculation of absorbed dose and EDE in the adult ORNL hermaphroditic phantom when using different computational models for generating the x-ray spectra.**

I. Introduction

Detailed knowledge of x-ray spectra is required for the mathematical modeling and optimization of imaging systems design in radiological imaging. The direct measurement of spectra, however, requires expensive equipment and requires careful attention and planning during the experimental measurement setup [1-2], which is generally not practicable in a clinical diagnostic radiology department with limited physics support. Since direct measurement of x-ray spectra is time-consuming and remains a difficult task, attempts for prediction of x-ray spectra in different energy ranges and various target/filter combinations have begun several decades ago and still represent an active research area. Generally the x-ray prediction models can be divided into three categories: empirical [3-4], semi-empirical [5-10] and Monte Carlo calculations [11-13]. The spectra predicted with the nominated models have not the same bremsstrahlung x-ray energy distribution and characteristic x-ray intensity, even for the same tube voltage and target angle. Thus, the accuracy of predicted spectra with these methods should be investigated considering the impact they might have on diagnostic radiological imaging system performance parameters and radiation dosimetry calculations.

In this study, the spectra generated by selected empirical (TASMIP and MASMIP) and semi-empirical (IPEM, XCOMP, X-rayb&m, X-raytbc, Blough et al. and Tucker et al.) models as well as Monte Carlo calculations (MCNP4C, EGS4 and ITS3.0) have been assessed in diagnostic radiology and mammography energy range through comparison with measured spectra published in Fewell et al. [1-2].

II. Materials and Methods

A. Measured Spectra

The reference spectra in diagnostic radiology energy range were taken from experimental measurements reported in the Handbook of Computed Tomography X-ray Spectra published by Fewell et al. [2] for Eimac (B-160-H, A-465) x-ray tube (Ohio Nuclear Inc., Solon, OH) with 12.5° tungsten target angle and nominal inherent filtration 1.2 mm Al_{eq}. The x-ray spectra were measured with high-purity germanium detector. The spectrometer was calibrated to give an energy conversion of 0.15 keV per channel. After correction of detector response, the x-ray spectra were tabulated with 2 keV energy bin.

The reference spectra in mammography energy range were selected from experimental measurements published in the Handbook of Mammography X-ray Spectra [1]. The tabulated spectra in 1 keV energy bin for Dynamax M64 molybdenum and Dynamax 69M tungsten target x-ray tube with inherent

This work was supported by Amirkabir University of Technology, Department of Physics & Nuclear Sciences and the Swiss National Science Foundation under grant SNSF 3152A0-102143.

M. R. Ay is with the Department of Physics & Nuclear Sciences, Amirkabir University of Technology, Tehran, Iran and Division of Nuclear Medicine, Geneva University Hospital, CH-1211 Geneva, Switzerland (e-mail: farshid.ay@tppgems.com)

S. Sarkar is with the Department of Medical Physics, Tehran University of Medical Science, Tehran, Iran

M. Shahriari is with the Department of Nuclear Engineering, Shahid Beheshti University, Tehran, Iran

D. Sardari is with the Department of Physics & Nuclear Sciences, Amirkabir University of Technology, Tehran, Iran

H. Zaidi is with the Division of Nuclear Medicine, Geneva University Hospital, CH-1211 Geneva, Switzerland (e-mail: habib.zaidi@hcuge.ch)

filtration 0.6 mm Al_{eq} and 12° target angle, were used as reference spectra in this study.

B. Computational Models

1) Empirical Models. This category of models is based on interpolating polynomials fitting of the measured data at each energy, without any assumption regarding the physics of x-ray production in the x-ray tube. TASMIP and MASMIP empirical models developed by Boone et al. were assessed in this study [3-4].

2) Semi-empirical Models. This category of models is based on a theoretical formulation to calculate the x-ray spectra by mathematical derivation followed by some tuning in the equations' parameters using measured spectra. The semi-empirical models investigated in this study included IPEM, XCOMP, X-rayb&m, X-raytbc, Blough et al. and Tucker et al. [5-10].

3) Monte Carlo Calculation. These models use direct Monte Carlo transport of electrons and generated photons in the target and filter for calculation of x-ray spectra. For the purpose of Monte Carlo simulation of x-ray spectrum, some groups used self-written or in house developed computer codes while others used public domain general-purpose Monte Carlo codes such as MCNP [11], EGS4 [12] and ITS [13]. These latter codes were used in this work. An in-depth description of the use of Monte Carlo calculations for x-ray spectra simulation is given elsewhere [14].

TABLE I
SUMMARY OF COMPUTATIONAL MODELS USED FOR GENERATION OF X-RAY SPECTRA IN RADIOLOGY AND MAMMOGRAPHY ENERGY RANGE.

Computational model	Category	Target Material	Reference
Measurement[R]	Experimental	W	Fewell et al. [2]
Measurement[M]	Experimental	W, Mo, W/Mo	Fewell et al. [1]
TASMIP[R,M]	Empirical	W	Boone et al. [3,4]
MASMIP[M]	Empirical	Mo	Boone et al. [4]
X-rayb&m[R,M]	Semi-empirical	W	Birch and Marshal [5]
IPEM[R,M]	Semi-empirical	W, Mo, Rh	Cranley et al. [8]
XCOMP[R,M]	Semi-empirical	W	Nowotny and Hofer [9]
X-raytbc[R,M]	Semi-empirical	W	Tucker et al. [6]
Tucker et al.[M]	Semi-empirical	Mo	Tucker et al. [7]
Blough et al.[M]	Semi-empirical	W, Mo, Rh	Blough et al. [10]
MCNP4C[R,M]	Monte Carlo	All materials	Briesmeister [11]
EGS4[R,M]	Monte Carlo	All materials	Nelson et al. [12]
ITS3.0[R,M]	Monte Carlo	All materials	Halbleib et al. [13]

[R]Radiology energy range
[M]Mammography energy range

C. Comparative Assessment Strategy

The calculated spectra using the different computational models summarized in Table I were assessed with measured spectra by comparing different figures of merit as described below.

1) Energy Spectra. The spectrum shape is the best parameter for qualitative visual assessment between two spectra. Quantitative evaluation of the differences between measured spectra and the spectra generated by different models was performed using statistical student's t-test analysis. Whereas, the spectra shape and beam quality is function of tube voltage, filtration and target angle, we have used exactly the same parameters as experimental measurement spectra for the generation of x-ray spectra using the different models.

2) Beam Quality. Attenuation curves and half value layers (HVLs) are standard indices of x-ray beam quality. The transmission curves were calculated by dividing the transmitted air kerma through the filter to the air kerma without the filter being present.

3) K x-ray Yield. The K x-ray yield indicates the contribution of characteristic x-rays to the spectra. This value is determined by subtracting the bremsstrahlung part of spectra from total detected photons in the desired region and normalizing to total number of photons in the spectra.

4) Absorbed Dose and EDE. The effect of using different computational models for the generation of x-ray spectra on the calculation of absorbed dose to the breasts and effective dose equivalent was investigated. The MCNP4C Monte Carlo code was used for calculation of absorbed dose in the adult ORNL hermaphroditic phantom using the different models investigated in this study.

III. RESULTS

A. Diagnostic Radiology

Fig. 1(a) shows the comparison of tungsten x-ray spectra calculated using semi-empirical models with measured spectrum at 100 kV, while the spectra illustrating empirical and Monte Carlo calculations are shown in Fig. 1(b). The spectra were normalized to total number of photons (unit area). According to Fig. 1(a), all semi-empirical models based on Birch and Marshal theory (IPEM, XCOMP and X-rayb&m) have lower intensity in low energies while they have a higher intensity in high energies (E>68 keV) in comparison with measured spectra. This behavior is observed for all tube voltages. The K x-ray yield in all peaks is higher than measured spectra for IPEM and XCOMP while these values are lower for X-rayb&m model. It has been shown that the X-raytbc model produces more low energy x-rays (E<42 keV) in comparison with measured spectra (Fig. 1a). The characteristic x-rays predicted with this model are lower than measured

spectra in all peaks and for all tube voltages. Good agreement was achieved between the measured bremsstrahlung x-ray spectra and the one produced by TASMIP model (Fig. 1b) while the characteristic x-rays have lower intensity. The spectra calculated by MCNP4C have higher intensity in low energy photons while this behavior is reversed for energies higher than 68 keV in comparison with measured spectra. The K x-ray yield has higher intensity for MCNP4C spectra in all energies whereas the low energy bremsstrahlung has higher intensity in the spectra simulated by EGS4.

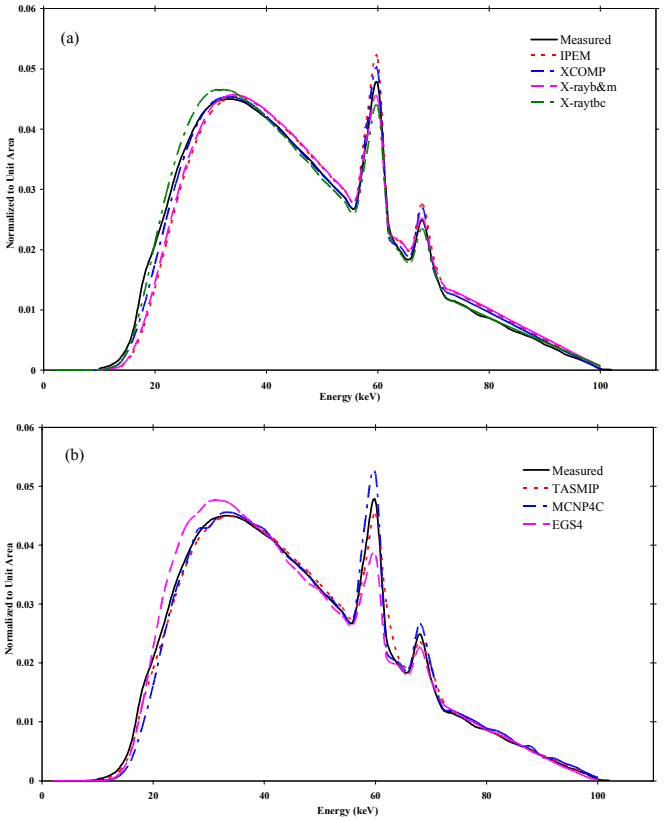

Fig. 1. Comparison of x-ray spectra generated using the different computational models with measured spectra at 100 kV tube voltage for 12.5° tungsten target, 1.2 mm Al_{eq} inherent filtration and FSD 127 cm. (a) Semi-empirical models; (b) Empirical and Monte Carlo models.

The spectra calculated with IPEM, XCOMP and X-rayb&m result in higher values of transmission curves in comparison with measured spectra for all tube voltages. This behavior is reversed for transmission curves calculated using X-raytbc, whereas there is good agreement between the measured transmission curves and those calculated using TASMIP. The transmission curves calculated with MCNP4C spectra generally have higher values, whereas, the EGS4 transmission curve have lower values in comparison with measured spectra. Table II shows the HVLs and EDE in ORNL hermaphroditic phantom for typical chest imaging setup calculated using different computational models at 100 kV.

B. *Mammography*

Fig. 2 shows the comparison of generated x-ray spectra by different computational models with measured spectra at 30 kV tube voltage. The spectra calculated using the different computational models have higher amplitude in the low energy range (E<15 keV) compared to measured spectra as a result of the normalization procedure. IPEM and MASMIP produce the same intensity at low energies. It was shown from the calculation of the difference in K x-ray yield for all peaks that MASMIP underestimates the production of characteristic x-rays while MCNP4C overestimates it. The highest difference in K x-ray yield was obtained for MCNP4C spectra even with different settings of the XNUM parameter. The spectra generated with all computational models underestimate the transmission curves. Table III shows the calculated HVL for spectra generated using different computational models at 30 kV. The maximum relative difference (12%) was observed for ITS3.0 spectra.

TABLE II

CALCULATION OF HVLS AND EFFECTIVE DOSE EQUIVALENT IN THE ADULT ORNL HERMAPHRODITIC PHANTOM FOR TYPICAL CHEST X-RAY IMAGING SETUP USING MCNP4C MONTE CARLO CALCULATIONS.

Computational	100 kV, 1.2 mm Al filter			
model	HVL (mm)	Diff (%)	EDE (μSv)	Diff (%)
Measured	2.29	na	40.00±1.4	na
IPEM	2.67	-16.5	41.30±1.4	-3.2
XCOMP	2.68	-17.0	40.55±1.4	-1.4
X-rayb&m	2.65	-15.7	41.11±1.5	-2.8
X-raytbc	2.22	3.0	40.00±1.6	0
TASMIP	2.29	0	40.37±1.5	-0.9
MCNP4C	2.40	-4.8	40.74±1.4	-1.8
EGS4	2.15	6.1	39.63±1.4	0.9

Fig. 3 shows the comparison of the spectra predicts by different models with measured spectra at 30 kV. The peak of calculated spectra occurred at lower energy in comparison with measured spectra and has lower amplitude. This behavior is reversed in lower and higher energies. The transmission curves obtained using all computational models have higher values in comparison with measured spectra at 30 kV. This behavior is reversed for 35 and 40 kV tube voltages. Table III summarizes the assessment of x-ray spectra quality and comparisons with measured spectra at 30 kV.

The MCNP4C-based Monte Carlo calculations of mean absorbed dose to the breasts ($\overline{D_b}$) in ORNL adult hermaphroditic phantom in typical mammography imaging setup when using different computational model for generating x-ray spectra at 30 kV are shown in Table III. The maximum difference in calculating $\overline{D_b}$ in molybdenum target is 2.5% for

Blough et al. model whereas this difference reduces to 1.5% for X-raytbc tungsten target model.

IV. Discussion

The different polynomial functions used in the semi-empirical models are the origin of the discrepancy between measured and calculated bremsstrahlung x-ray energy distribution obtained. The comparison of these functions showed that the Birch and Marshal model (IPEM, XCOMP and X-rayb&m) produce less low energy photons and more high energy photons than X-raytbc model [15]. The different target geometry used in these models should be considered especially for low energy photons. The spectra predicted by TASMIP empirical model in Fig. 1(b) has excellent agreement with measured spectra. The difference in K x-rays intensity is due to binning the data in 2 keV energy bins.

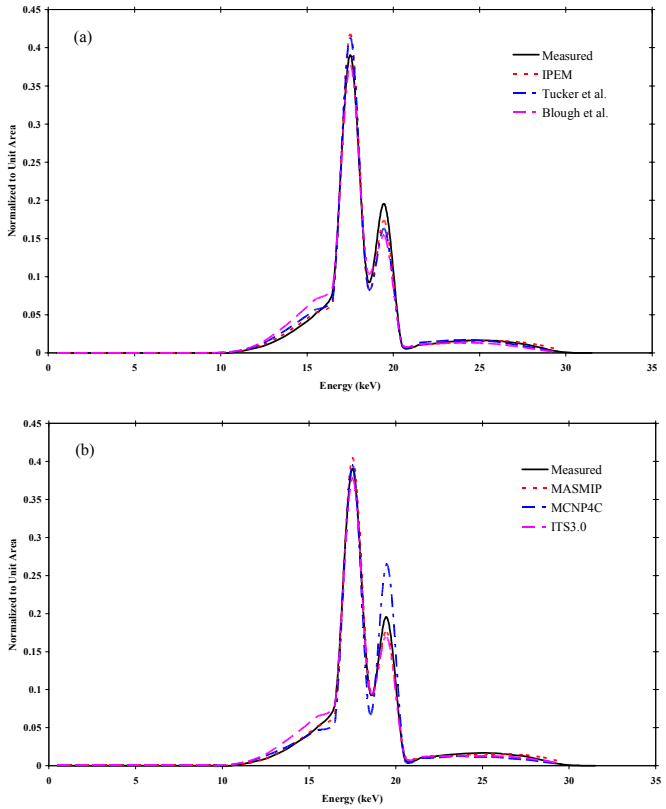

Fig. 2. Comparison of x-ray spectra generated using the different computational models with measured spectra at 30 kV tube voltage for 12° molybdenum target, 0.6 mm Al_{eq} inherent filtration, 0.03 mm Mo additional filter and FSD 100 cm. (a) Semi-empirical models; (b) empirical and Monte Carlo models.

It should, however, be noticed that the measured spectra serving as reference in this work were used to derive the interpolating polynomials for this model, which might bias the conclusions drawn from this comparison.

The intensity of K x-rays in the spectra is another important parameter, which should be considered in the comparison of different computational models.

The semi-empirical models use an empirical relationship to determine the intensity of K x-rays, however, they rely on measured spectra for adjusting the intensity of characteristic x-rays. Although the same measured spectra were used for adjusting the characteristic x-rays in X-raytbc and X-rayb&m, the lower intensity in X-raytbc is the result of target absorption because of higher attenuation of x-rays in this model. Characteristic photons in MCNP4C are created by the electron impact ionization (EII) process. However, the model overestimates the total number of EII characteristic photons especially in mammography energy range. The low characteristic x-rays intensity in EGS4 spectra can be explained by the fact that the contribution of electron impact ionization had not been included in the EGS4 code system at the time of simulation. All semi-empirical models based on Birch and Marshal theory (IPEM, XCOMP and X-rayb&m) [5] produce spectra with higher quality Compared to measured spectra, while the situation is reversed for the model based on Tucker et al. theory (X-raytbc) [6]. This is due to production of softer x-ray spectra in Tucker et al. model. The transmission curves calculated from MCNP4C spectra are higher than measured spectra owing to the overestimation of K x-rays and high energy bremsstrahlung photons (E>68 keV). The EGS4 spectra produce lower transmission curves compared to measured spectra as a result of underestimation of K x-rays.

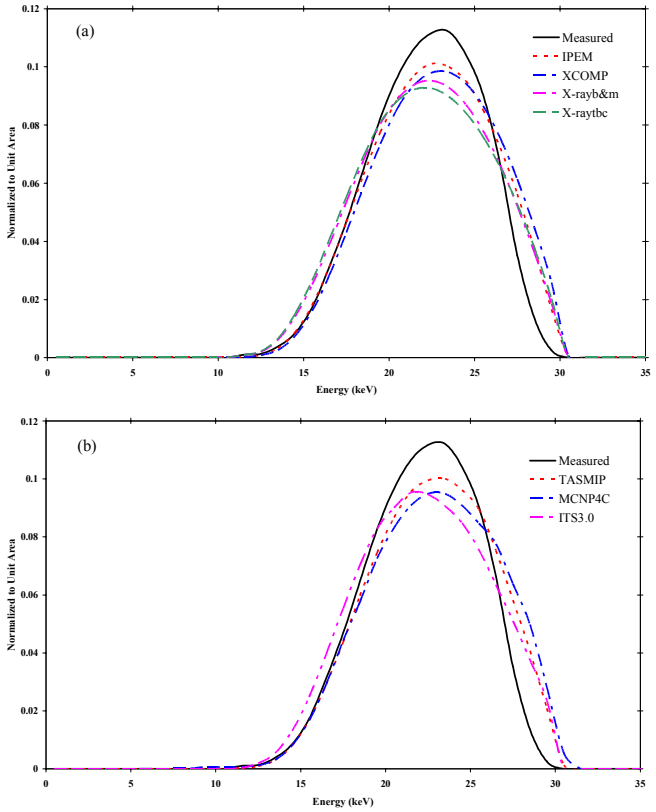

Fig. 3. Comparison of x-ray spectra generated using the different computational models with measured spectra at tube voltage 30 kV for 12° tungsten target, 0.6 mm Al_{eq} inherent filtration, 1.02 mm Al additional filter and FSD 100 cm. (a) Semi-empirical models; (b) empirical and Monte Carlo models.

The calculation of absorbed dose and EDE in the adult ORNL hermaphroditic phantom using as input the spectra generated with different models allowed to assess the influence of the predicted spectra for radiation dosimetry applications. The calculated EDE from X-raytbc model is lower than estimates resulting from the application of other models and has excellent agreement with measured spectra.

The comparative assessment of x-ray spectra produced with different computational models with measured spectra for molybdenum target showed that Blough et al. and Tucker et al. models produce higher soft energy than IPEM for the reasons discussed above for semi-empirical models. The difference between measured and MASMIP spectra can be attributed to the fact that different measured spectra have been used for derivation of interpolating polynomials [4]. The comparison of MCNP4C spectra with measured spectra revealed that this code highly overestimates the production of K x-rays as reported in a recent publication [14]. According to Fig. 3, the spectra peak in all semi-empirical models occurred in lower energy and with less intensity than measured spectra. One plausible explanation could be the overestimation of electrons penetration in the target in Tomson-Whiddington relation [5].

TABLE III

CALCULATION OF HVLS AND MEAN ABSORBED DOSE TO THE BREASTS ($\overline{D_b}$) IN THE ADULT ORNL HERMAPHRODITIC PHANTOM FOR TYPICAL MAMMOGRAPHY IMAGING SETUP.

Computational	Mo Target				W Target			
model	HVL (mm)	Diff (%)	$\overline{D_b}$(mGy)	Diff (%)	HVL (mm)	Diff (%)	$\overline{D_b}$(mGy)	Diff (%)
Measured	0.50	na	2.00	na	0.81	na	2.00	na
IPEM	0.47	6.0	1.99	0.5	0.80	1.2	2.00	0
Blough et al.	0.47	6.0	1.95	2.5	-	-	-	-
Tucker et al.	0.46	8.0	1.97	1.5	-	-	-	-
MASMIP	0.47	6.0	2.00	0.0	-	-	-	-
MCNP4C	0.48	4.0	2.00	0.0	0.81	0	2.01	-0.5
ITS3.0	0.44	12.0	1.96	2.0	0.74	8.6	1.98	1.0
XCOMP	-	-	-	-	0.80	1.2	2.01	-0.5
X-rayb&m	-	-	-	-	0.84	-3.7	1.98	1.0
X-raytbc	-	-	-	-	0.82	-1.2	1.97	1.5
TASMIP	-	-	-	-	0.81	0	2.01	-0.5

V. CONCLUSION

The spectra generated using different computational models have been verified against measured spectra. The student's t-test statistical analysis didn't reveal statistically significant differences between measured and generated spectra. The energy distribution and the quality of spectra produced by X-raytbc model has better agreement with measured spectra than other models in diagnostic radiology energy range, while the IPEM report No. 78 has better agreement in mammography energy range. There is no discernable discrepancy in the calculation of effective dose equivalent and mean absorbed dose to the breasts of the adult ORNL hermaphroditic phantom in typical x-ray chest imaging and mammography setup when using spectra generated with different computational models.

ACKNOWLEDGMENT

The authors would like to thank Drs J.M. Boone, M. Bhat, K.P. Ng, L.E. Wilkinson, G. Stirling, R. Nowotny and G.W. Allen who shared with us their data and programs.

REFERENCE

[1] T. R. Fewell and R. E. Shuping, "Handbook of mammography spectra," HEW Publication, FDA, Washington, DC, 79-8071, Oct. 1978.

[2] T. R. Fewell, R. E. Shuping and K. E. Heaty, "Handbook of computed tomography x-ray spectra," HHS Publication, FDA, Washington, DC, 81-8162, Apr. 1981.

[3] J. M. Boone and J. A. Seibert, "An accurate method for computer-generating tungsten anode x-ray spectra from 30 to 140 kV," *Med. Phys.* vol. 24, no. 11, pp. 1661-1670, 1997.

[4] J. M. Boone, T. R. Fewell and R. J. Jennings, "Molybdenum, rhodium and tungsten anode spectral models using interpolating polynomials with application to mammography," *Med. Phys*. vol. 24, no. 12, pp. 1863-1847, 1997.

[5] R. Birch and M. Marshall, "Computation of bremsstrahlung x-ray spectra and comparison with spectra measured with a Ge(Li) detector," *Phys. Med. Biol.* vol. 24, no. 3, pp. 505-517, 1979.

[6] D. M. Tucker, G. T. Barnes and D. P. Chakraborty, "Semiempirical model for generating tungsten target x-ray spectra," *Med. Phys.* vol. 18, no. 2, pp. 211-218, 1991.

[7] D. M. Tucker, G. T. Barnes and X. Wu, "Molybdenum target x-ray spectra: a semiempirical model," *Med. Phys.* vol. 18, no. 3, pp. 402-407, 1991.

[8] K. Cranley, B. J. Gilmore, G. W. A. Fogarty and L. Desponds, "Catalogue of diagnostic x-ray spectra and other data," The Institute of Physics and Engineering in Medicine (IPEM), York, UK, Rep. no. 78, 1997.

[9] R. Nowotny and A. Hofer, "Ein program fur die berechnung von diagnostischen ronttgenspektren," *Fortschr. Rontgenstr.* vol. 142, pp. 1309-1318, 1985.

[10] M. M. Blough, R. G. Waggener, W. H. Payne and J. A. Terry, "Calculated mammographic spectra confirmed with attenuation curves for molybdenum, rhodium, and tungsten targets," *Med. Phys.* vol. 25, no. 9, pp. 1605-1612, 1998.

[11] J. F. Briesmeister, "MCNP- A general Monte Carlo N-particles transport code," Los Alamos National Laboratory, Los Alamos, NM, 2000.

[12] W. R. Nelson, H. Hirayama and D. Rogers, "The EGS4 code system,", Stamford Linear Accelerator, Stanford, 1985.

[13] J. A. Halbleib, R. P. Kensek, T. A. Mehlhorn, G. D. Valdez, S. M. Seltzer and M. J. Berger, "ITS version 3.0: The Integrated TIGER Series of couple electron /photon Monte Carlo transport code," Sandia National Laboratories, Albuquerque, 1992.

[14] M. R. Ay, M. Shahriari, S. Sarkar, M. Adib and H. Zaidi, "Monte Carlo simulation of x-ray spectra in diagnostic radiology and mammography using MCNP4C*," Phys. Med. Biol.* vol. 49, pp. 4897-4917, 2004.

[15] J. P. Bissonnette and L. J. Schreiner, "A comparison of semi-empirical models for generating tungsten target x-ray spectra," *Med. Phys.* vol. 19, no. 3, pp. 579-582, 1992.